Expression of Multidrug Resistance-Associated Protein (MRP) in Human Retinal Pigment Epithelial Cells and Its Interaction with BAPSG, a Novel Aldose Reductase Inhibitor

Jithan V. Aukunuru,[1] Gangadhar Sunkara,[1] Nagesh Bandi,[1] Wallace B. Thoreson,[2] and Uday B. Kompella[1,2,3]

Received January 17, 2001; accepted January 22, 2001

Purpose. The objective of this study was to determine the expression and activity of multidrug resistance-associated protein (MRP) in the retinal pigment epithelial (RPE) cells and to further assess whether BAPSG, a novel anionic aldose reductase inhibitor, interacts with MRP.

Methods. Functional and biochemical evidence for MRP was obtained in a human retinal pigment epithelial (ARPE-19) cell line and primary cultures of human retinal pigment epithelial (HRPE) cells. Fluorescein accumulation and efflux in the presence and absence of MRP inhibitors was used to obtain functional evidence for MRP. Western blots and RT-PCR were used to obtain biochemical evidence for MRP1. The influence of MRP inhibitors on BAPSG accumulation and efflux in ARPE-19 cells was determined to understand its interaction with MRP.

Results. MRP inhibitors increased fluorescein accumulation and reduced efflux in RPE cells. Both cell types exhibited a 190-kDa western blot band corresponding to MRP1 protein and a 287 bp RT-PCR band corresponding to MRP1 mRNA. MRP inhibitors reduced BAPSG efflux and increased its accumulation in ARPE-19 cells.

Conclusions. MRP is functionally and biochemically active in human RPE cells. Anionic BAPSG is a likely substrate for MRP.

KEY WORDS: aldose reductase inhibitor; Fluorescein; MRP; RPE cells.

INTRODUCTION

The retinal pigment epithelium (RPE) is a monolayer between the neural retina and choroid and supports the function of the photoreceptors. RPE expresses various ion transporters, amino acid transporters, myo-inositol transporter, ascorbic acid transporter, and probenecid-sensitive organic anion transporter (1,2). These transporters regulate the uptake of ions and solutes into and across this layer. Although a probenecid sensitive organic anion transporter has been suggested in RPE cells (2), no reports exist regarding the presence of multidrug resistance-associated protein (MRP), an organic anion efflux pump.

MRP transporters are members of the ATP-binding cassette (ABC) superfamily of transport systems and function as ATP-dependent drug efflux pumps in cancer cells as well as normal cells (3). Six different genes coding for MRPs, (MRP1 through MRP6), have been identified thus far (4,5). Previous studies demonstrated that MRP exports organic anions and glucuronide, glutathione, or sulfate conjugated compounds (6). MRP is expressed in blood-brain barrier and blood-CSF barrier (7–9). RPE cells forming inner blood-retinal barrier are similar to blood-brain barrier in their function and therefore, it is likely that drug efflux proteins such as MRP are expressed in this epithelium. MRP, if present in RPE cells, is likely to reduce the accumulation of anionic drugs.

In this study, we obtained evidence for the presence of MRP in primary cultures of human retinal pigment epithelial cells (HRPE) as well as a human retinal pigment epithelial cell line (ARPE-19). ARPE-19 is a cell line developed from RPE cells obtained from a male donor (10). ARPE-19 cells have structural and functional properties characteristic of RPE cells *in vivo* (11). Also, ARPE-19 cells exhibit polarized distribution of cell surface markers and this cell line has been proposed as a suitable model for RPE cells (12).

The RPE is the target for many pharmacological agents in pathological conditions including proliferative vitreoretinopathy, diabetic retinopathy, and macular degeneration. Aldose reductase inhibitors (ARIs) are potential therapeutic agents for diabetic retinopathy as they are capable of reducing vitreous levels of vascular endothelial growth factor (VEGF) (13), a potent mitogen associated with retinal neovascularization, secreted by RPE cells (14). BAPSG (N[4-(benzoylamino)phenyl sulfonyl]glycine) is a selective ARI with an IC_{50} value of 0.4 μM as estimated using rat lens aldose reductase (15). With a pKa value of 3.35, it is an anion at physiological pH. Since we obtained evidence for the ability of BAPSG to reduce VEGF secretion from RPE cells (16), it is a candidate for the retinal delivery during diabetic retinopathy. Because BAPSG is an organic anion and because the cellular accumulation of anions exported by MRP can be enhanced by co-treatment with MRP inhibitors (17), we determined this possibility for BAPSG in the current study.

MATERIALS AND METHODS

Materials

Calcium chloride, 2,4-dinitrophenol, fluorescein, glucose, HEPES, indomethacin, magnesium sulfate, probenecid, sodium bicarbonate, sodium chloride, sodium azide, and verapamil were obtained from Sigma Chemical Co. (St. Louis, MO).

Cell Culture

ARPE-19 cells were obtained from ATCC (Rockville, MD). Primary cultures of human retinal pigment epithelium were prepared as described by Thoreson *et al.* (18). Both the cell types, grown in 75 cm^2 cell culture flasks (Becton Dickinson Labware, Franklin Lakes, NJ), were cultured in 1:1 DMEM/F12 medium (Gibco, Grand Island, NY) with 56 mM of sodium bicarbonate, 2 mM L-glutamine, 15 mM HEPES buffer, 10% (ARPE-19) or 20% (HRPE) fetal bovine serum (Gibco), and 1% penicillin G (100 I.U./ml)/ streptomycin (100 μg/ml) solution (Gibco). For the accumulation and efflux

[1] Department of Pharmaceutical Sciences, University of Nebraska Medical Center, Omaha, Nebraska 68198-6025.
[2] Department of Ophthalmology, University of Nebraska Medical Center, Omaha, Nebraska 68198-6025.
[3] To whom correspondence should be addressed. (e-mail: ukompell@unmc.edu)

studies, day 6 or 7 cells grown in 48-well tissue culture plates (Becton Dickinson) at a seeding density of 1.66 X 10^5 cells/cm^2 were used. ARPE-19 and HRPE cells were used between passages 19–29 and 2–4, respectively. Lysates of MRP1 expressing PANC-1 cells, a gift from Dr. Donald Miller of University of Nebraska Medical Center, was used as a positive control in western blot studies. The western blot and RT-PCR studies were performed with day 6 or 7 cells cultured in 75 cm^2 flasks.

Fluorescein and BAPSG Accumulation

Effect of Metabolic Inhibitors and Low Temperature

Cellular accumulation studies were performed using assay buffer (pH 7.4) of the following composition: NaCl (122 mM), $NaHCO_3$ (25 mM), $MgSO_4$ (1.2 mM), K_2HPO_4 (0.4 mM), $CaCl_2$ (1.4 mM), HEPES (10 mM), and glucose (10 mM). To determine the energy-dependency of fluorescein and BAPSG accumulation, after pre-equilibrating ARPE-19 cell monolayers with assay buffer for 30 min at 37°C, the assay buffer was replaced with either fluorescein (10, 50, 100, and 200 μM) or BAPSG (10, 50, 100, and 200 μM) solutions in assay buffer with and without metabolic inhibitors, 2,4-dinitrophenol (1 mM) and sodium azide (10 mM). Also, solute accumulation without metabolic inhibitors was determined at 4°C. In all these studies, at the end of 3-h solute accumulation, the solutions were aspirated and the monolayers were washed thrice with 1.0 ml of ice-cold PBS. Subsequently, the cell monolayers were solubilized with 0.5 ml of 1% Triton-X solution in PBS using a shaker incubator maintained at 37°C. Fluorescein in all the cell lysates was analyzed using a spectrofluorometer with excitation and emission wavelengths set at 488 and 510 nm, respectively. Protein content in the cell lysates was estimated using a BioRad (Hercules, CA) or Pierce (Rockford, IL) protein assay kit. The amount of fluorescein in samples was normalized to protein content in each sample.

For BAPSG analysis, the cell lysates were freeze-dried and BAPSG was extracted from these lyophilized cell lysates. To extract BAPSG, 200 μl of acetonitrile:methanol (50:50) was added to the freeze-dried product and placed for 6 h in a shaking incubator maintained at 20°C. The samples were vortexed for 5 min before centrifuging at 3000 *g* for 10 min. The supernatant was collected and the amount of BAPSG was determined using a reverse-phase HPLC method as described previously (19). The BAPSG levels were normalized to the protein content in the cell lysates.

Influence of MRP Inhibitors

To determine the effect of various concentrations of MRP inhibitors on fluorescein and BAPSG accumulation, ARPE-19 or HRPE cell monolayers were pre-equilibrated with assay buffer for 30 min at 37°C, and then the assay buffer was replaced with either fluorescein (100 μM) or BAPSG (100 μM) solution with or without indomethacin (10, 50, and 100 μM), probenecid (100, 500, and 1000 μM), and verapamil (10, 50, and 100 μM). Indomethacin (20,21), probenecid (22,23), and verapamil (24) were previously shown to inhibit MRP. After allowing fluorescein or BAPSG accumulation for 1, 3, or 6 h, cell monolayers were washed with ice-cold PBS, lysed, and fluorescein and BAPSG were estimated as per the methods described above.

Fluorescein and BAPSG Efflux

Following a 3-h accumulation period, the fluorescein (100 μM) and BAPSG (100 μM) solutions were removed and the monolayers were washed twice with the assay buffer. Then, the efflux of fluorescein and BAPSG into assay buffer with or without indomethacin (10 μM), probenecid (100 μM) and verapamil (100 μM) was assessed for 1, 2, and 3 h. At the end of the efflux study, the cell monolayers were solubilized with 0.5 ml of 1% Triton-X solution in PBS and the protein content was determined. Fluorescein and BAPSG in the efflux medium were analyzed using a spectrofluorometer and a HPLC with UV detection, respectively. The amounts of fluorescein and BAPSG were normalized to protein content in each lysate.

Western Blot Analysis for MRP1 Protein Expression

HRPE, ARPE-19 and PANC-1 (positive controls) cell monolayers were solubilized in phosphate buffered saline (pH 7.4) containing 1% SDS and protease inhibitors (Boehringer Mannheim, Indianapolis, IN). These cell lysates were loaded at a protein content of 10 μg onto pre-formed 7.5 % polyacrylamide gels (Bio-Rad, Hercules, CA) and the proteins were separated using SDS-PAGE. Molecular weight markers ranging from 220 to 14.3 kDa (Amersham Life Science, Inc., Arlington Heights, IL) were used to identify the corresponding band of MRP1. The gels were run at 40 V for 30 min and then continued at 70 V for another h. The proteins were then transferred onto polyvinylidene fluoride (PVDF) membranes (Millipore, Bedford, MA) using a current of 480 mA. The PVDF membrane was washed with the blocking buffer containing 0.3% Tween-20 and 1% BSA and incubated overnight at 4°C with the MRP1 antibody, MRPm6 (Kamiya, Seattle, WA). The antibody was used at (1:100) dilution. After a series of washes with the blocking buffers, a secondary horseradish peroxidase mouse IgG antibody (Amersham Life Science, Inc.) was added (1:1500) and incubated at 4°C for one h. The specific protein bands were visualized using a chemiluminescence kit (Amersham Life Science, Inc.).

RT-PCR Analysis for MRP1 mRNA Expression

Using RT-PCR, MRP1 expression was identified in ARPE-19 and HRPE cells using the Access RT-PCR System (Promega Corporation, Madison, WI). In brief, total RNA was extracted from confluent ARPE-19 and HRPE cells using RNA STAT-60™ RNA isolation kit (TEL-TEST, Friendswood, TX) as per the manufacturer's recommendations. RT-PCR for both cell types was performed in a standard 50 μl reaction mixture containing 5 units of Tfl DNA polymerase, 5 units of AMV reverse transcriptase, 20 pmoles each of sense and antisense primer, 0.2 mM deoxytriphosphate nucleotides, and 2 mM $MgCl_2$. Amplification of the cDNA was performed using MRP1 specific primers as previously described (25). The amplified products were separated on a 3% agarose gel and visualized by staining with ethidium bromide.

MTT Assay

ARPE-19 cells, plated at a density of 3×10^3 cells/well in 96-well microtiter plates, were incubated on day 6 with fluo-

rescein and various inhibitors. Cell viability was determined with the colorimetric MTT assay. Briefly, at the end of the incubation period, 30 μl of MTT (Sigma Chemical Co.) solution [5 mg/ml in phosphate buffered saline (PBS)] was added to each well and incubated for 4 h at 37°C. The plates were shaken for 5 min to separate non-adherent and loosely attached cells. After carefully aspirating the supernatant, 100 μl of 0.04 N HCl in isopropanol was added to monolayer in each well to dissolve the dark blue crystals. The plates were shaken for 5 min to completely dissolve all the crystals. The absorbance was measured using a test wavelength of 560 nm and a reference wavelength of 630 nm using a microplate reader (BT 2000 Microkinetics, Fisher Biotech). The percentage of viable cells with the inhibitors was calculated relative to untreated cells.

Statistical Analysis

Student's t-test was used to evaluate the significance of differences between groups. $p < 0.05$ was considered statistically significant.

RESULTS

Evidence for MRP Activity

Fluorescein Accumulation: Influence of Low Temperature and Metabolic Inhibitors

At 37°C as well as 4°C, fluorescein accumulation in ARPE-19 cells increased significantly with increasing concentrations (Fig. 1). At 50 μM and above, fluorescein accumulation was significantly higher at 37°C compared to 4°C. At 37°C, while sodium azide significantly increased the accumulation of 10 and 50 μM fluorescein, dinitrophenol significantly increased the accumulation of 10 μM fluorescein. At 100 μM fluorescein and above, neither of the metabolic inhibitors significantly altered fluorescein accumulation.

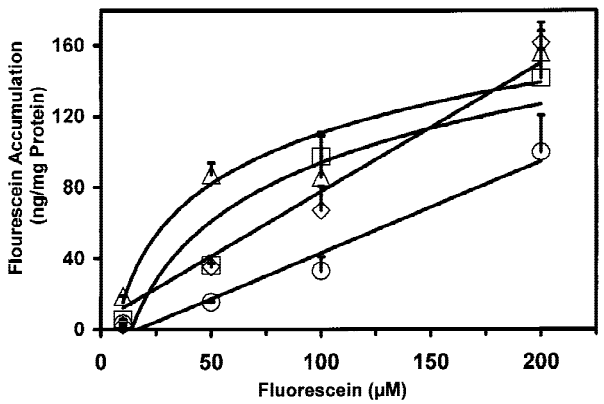

Fig. 1. Effect of low temperature and cellular energy depletors on fluorescein accumulation in ARPE-19 cells. Fluorescein at 10, 50, 100, and 200 μM was exposed for 3 h to ARPE-19 cells either alone at 4°C or at 37°C with or without 2,4-dinitrophenol (1 mM) and sodium azide (10 mM). At the end of the study, the cells were lysed and fluorescein was estimated. Key: ◇ = 37°C; □ = 2,4-dinitrophenol; △ = Sodium azide; ○ = 4°C. Data is expressed as mean ± S.D. for $n = 4$.

Fluorescein Accumulation: Influence of MRP Inhibitors

Fluorescein accumulation in ARPE-19 and HRPE cells with and without MRP inhibitors is shown in Fig. 2. In general, in both cell types, fluorescein accumulation with MRP inhibitors was higher than the controls. In ARPE-19 cells (Figs. 2A, 2B, and 2C), indomethacin increased fluorescein accumulation at all concentrations and time-points except at 6 h with 100 μM indomethacin. All concentrations of probenecid at 1 h and 1 mM probenecid at 6 h increased fluorescein accumulation significantly. While 10 μM verapamil was ineffective at all time-points, 50 μM verapamil at 1 h and 100 μM verapamil at 6 h significantly increased fluorescein accumulation in ARPE-19 cells. In HRPE cells (Figs. 2D, 2E, and 2F), all inhibitors and concentrations significantly increased fuorescein accumulation at 3 and 6 h, except 10 μM verapamil at 6 h. At 1 h, none of the inhibitors significantly elevated fluorescein accumulation.

Fluorescein Efflux

Fluorescein efflux from control ARPE-19 cells was significantly higher at 2 and 3 h when compared to the efflux in the presence of MRP inhibitors (Fig. 3). The efflux at the end of 3 h was significantly decreased by 54, 45, and 60% in the presence of indomethacin, probenecid and verapamil, respectively.

Western Blot for MRP1 Protein Expression

An approximately 190-kDa protein band corresponding to MRP1 (Fig. 4A) was observed in HRPE (Lanes 1–4) and ARPE-19 (Lanes 6–9) cell lysates similar to the lysates of PANC-1 cells (Lane 5).

RT-PCR for MRP1 mRNA Expression

Using RT-PCR technique, RNA isolated from ARPE-19 and HRPE cells was examined for MRP1 mRNA expression (Fig. 4B). The results indicated a single band at 287 bp corresponding to MRP1 mRNA in ARPE-19 (Lanes 2) and HRPE (Lane 3) cells. Lane 4 with no bands corresponds to a negative control, a sample with no RNA template. The completion of RT-PCR reaction was confirmed by the amplification of a kit RNA template, a positive control, which gives a band at 330 bp (Lane 5).

Interaction of BAPSG With MRP

BAPSG Accumulation: Influence of Low Temperature and Metabolic Inhibitors

At both 37°C and 4°C, the accumulation of BAPSG in ARPE-19 cells increased with increasing concentrations of BAPSG (Fig. 5). The cellular accumulation was lower at 4°C compared to 37°C, with the differences being significant with 100 and 200 μM BAPSG. Although dinitrophenol and sodium azide increased BAPSG accumulation at most concentrations tested, significant increase was observed only with 10 μM BAPSG.

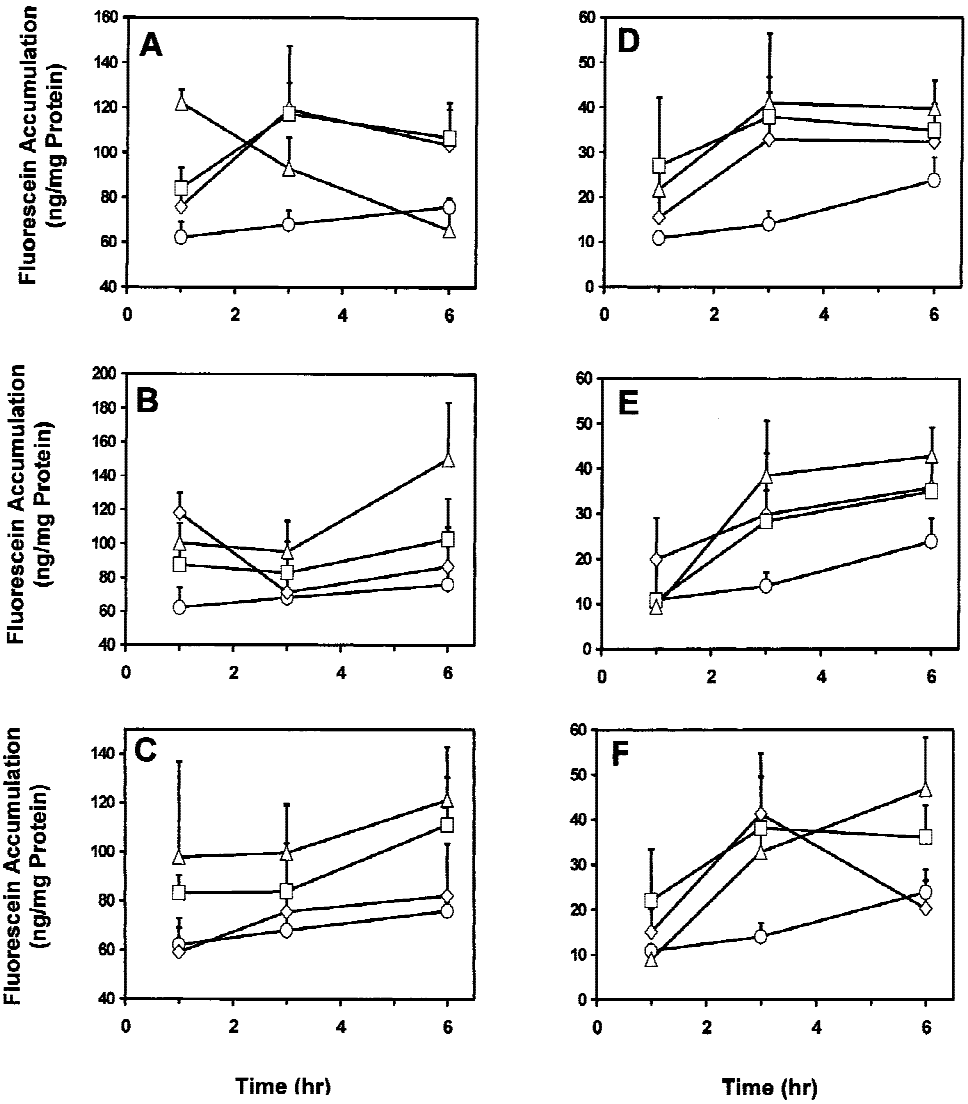

Fig. 2. Fluorescein accumulation in the presence and absence of MRP inhibitors. Key: A, B, C: Fluorescein accumulation in ARPE-19 cells. D, E, F: Fluorescein accumulation in HRPE cells. A, D: Indomethacin (○ = Control; ◇ = 10 μM; □ = 50 μM; △ = 100 μM), B, E: Probenecid (○ = Control; ◇ = 100 μM; □ = 500 μM; △ = 1000 μM), and C, F: Verapamil (○ = Control; ◇ = 10 μM; □ = 50 μM; △ = 100 μM). Fluorescein at 100 μM was exposed with or without varying concentrations of MRP inhibitors for 1, 3, or 6 h. At the end of the study, the cells were lysed and fluorescein was estimated. Data is expressed as mean ± S.D. for $n = 4$.

BAPSG Accumulation: Influence of MRP Inhibitors

BAPSG accumulation in ARPE-19 cells with and without MRP inhibitors is shown in Fig. 6. With increasing time of incubation, BAPSG accumulation increased in ARPE-19 cells. Also, the cellular accumulation was the lowest in controls among various treatments. Indomethacin and probenecid significantly increased BAPSG accumulation at all tested concentrations and time-points. Verapamil was not effective at 10 μM at all time-points. However, higher concentrations of verapamil significantly increased BAPSG accumulation at 1 and 3 h.

BAPSG Efflux

BAPSG efflux from control ARPE-19 cells at 2 and 3 h was significantly higher when compared to the efflux in the presence of all three MRP inhibitors (Fig. 7). The efflux at the end of 3 h was significantly decreased by 57, 64, and 52% in the presence of indomethacin, probenecid and verapamil, respectively.

MTT Assay

The results of MTT assay are shown in Table I. There was no significant difference in the viability of the cells between the control and the inhibitor treated groups.

DISCUSSION

We obtained functional evidence for the presence of MRP based on the accumulation and efflux of fluorescein, an anionic substrate for MRP (26,9). Three previously demonstrated MRP inhibitors increased fluorescein accumulation (Fig. 2) and reduced its efflux from RPE cells (Fig. 3), without affecting cell viability (Table I). Thus, an organic anionic efflux consistent with MRP activity is present in RPE cells. As

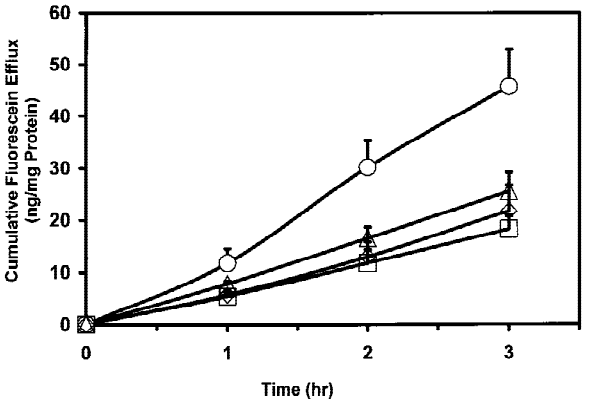

Fig. 3. Cumulative fluorescein efflux from ARPE-19 cells in the presence and absence of MRP inhibitors. Cells were exposed to 100 μM fluorescein for 3 h followed by efflux into assay buffer with MRP inhibitors. Indomethacin, probenecid, and verapamil were used at 10, 100, and 100 μM, respectively. Key: ○ = Control; ◇ = Indomethacin; □ = Probenecid; △ = Verapamil. Data is expressed as mean ± S.D for $n = 4$.

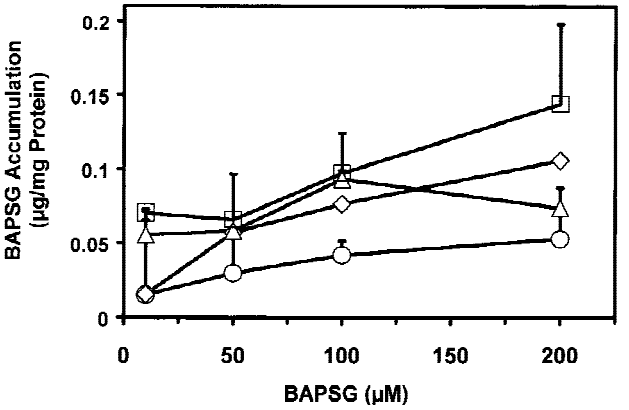

Fig. 5. Effect of low temperature and cellular energy depletors on BAPSG accumulation in ARPE-19 cells. BAPSG at 10, 50, 100, and 200 μM was exposed for 3 h either alone at 4°C or at 37°C with or without 2,4-dinitrophenol (1 mM) and sodium azide (10 mM). At the end of the study, the cells were lysed and BAPSG was estimated. Key: ◇ = 37°C; □ = 2,4-dinitrophenol; △ = Sodium azide; ○ = 4°C . Data is expressed as mean ± S.E.M. for $n = 4$.

fluorescein accumulation was reduced following transfection of MRP1 in MDCKII cells (26), our results are consistent with the presence of MRP1 activity in RPE cells. However, as the selectivity of fluorescein and MRP inhibitors for various MRPs has yet to be established, the contribution of other MRPs to the observed fluorescein efflux can not be ruled out.

We obtained two lines of biochemical evidence for the expression of MRP1 in ARPE-19 and HRPE cells. The first evidence was based on western blots using an MRP1 specific antibody (MRPm6). This antibody was previously reported (27) not to cross-react with MRP2, MRP3, and MRP5. Also, based on the sequence differences of MRPs, Scheffer *et al.* (27) suggested that MRPm6 is unlikely to cross-react with MRP4 or MRP6. Indeed, MRPm6 antibody was previously used to demonstrate the expression of MRP1 in PANC-1 cells (20). Using MRPm6 in western blots, we identified a 190-kDa band corresponding to MRP1 in ARPE-19 and HRPE cells

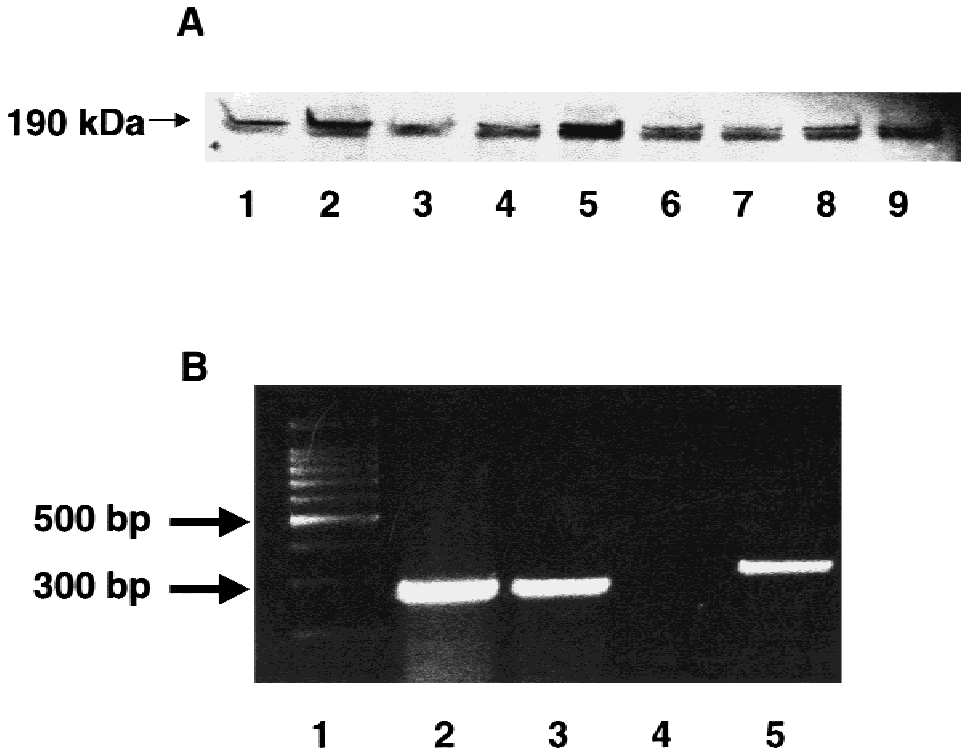

Fig. 4. A. Western blot analysis of MRP1 in RPE cells. Aliquots with ten micrograms of protein were loaded into each lane. Key: Lanes 1, 2, 3, 4: HRPE cells, Lane 5: positive control, Lanes 6, 7, 8, 9: ARPE -19 cells. B. RT-PCR analysis of MRP1 in RPE cells. Aliquots of 3 μg total RNA was subjected to RT-PCR. The samples were run on a 3% agarose gel and visualized using ethidium bromide. Key: Lane 1: Markers; Lane 2: ARPE-19 cells; Lane 3: HRPE cells; Lane 4: Negative control; and Lane 5: Kit control.

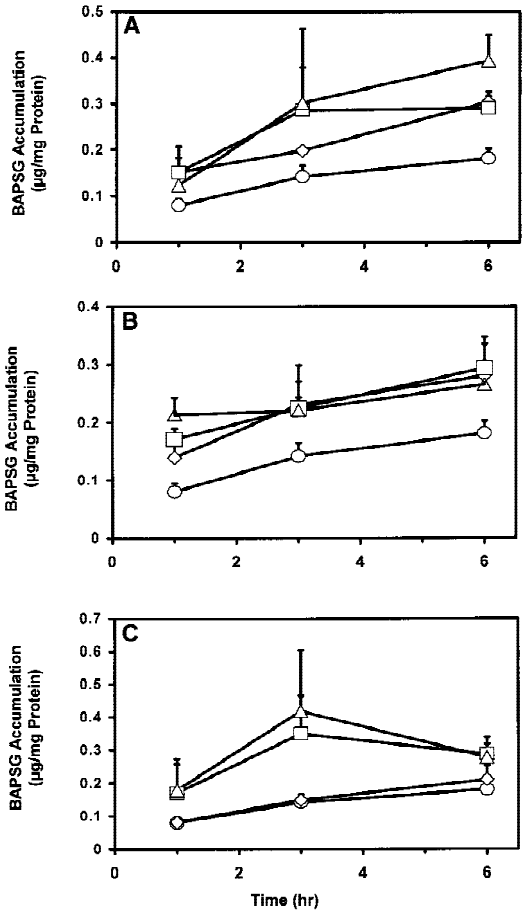

Fig. 6. BAPSG accumulation in ARPE-19 in the presence and absence of MRP inhibitors. A. Indomethacin (○ = Control; ◇ = 10 µM; □ = 50 µM; △ = 100 µM), B. Probenecid (○ = Control; ◇ = 100 µM; □ = 500 µM; △ = 1000 µM), C. Verapamil (○ = Control; ◇ = 10 µM; □ = 50 µM; △ = 100 µM). BAPSG at 100 µM was exposed with or without varying concentrations of MRP inhibitors for 1, 2, or 3 h. Data is expressed as mean ± S.D. for $n = 4$.

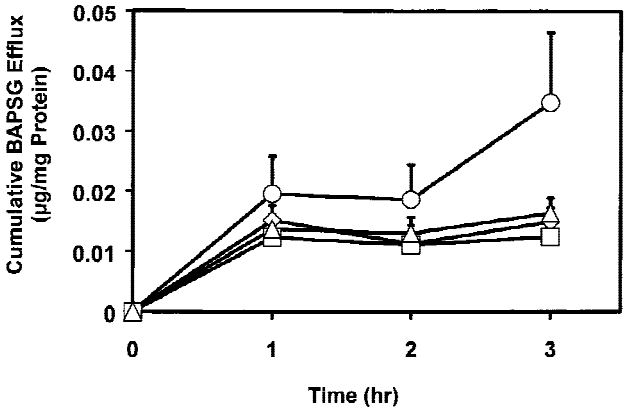

Fig. 7. Cumulative BAPSG efflux from ARPE-19 cells in the presence and absence of MRP inhibitors. Cells were exposed to either 100 µM BAPSG for 3 h followed by efflux into assay buffer with MRP inhibitors. Indomethacin, probenecid, and verapamil were used at 10, 100, and 100 µM, respectively. Key: ○ = Control; ◇ = Indomethacin; □ = Probenecid; △ = Verapamil. Data is expressed as mean ± S.D for n = 4.

(Fig. 4A). As a second biochemical evidence for MRP1, we demonstrated the presence of a 287-bp band corresponding to MRP1 mRNA in both these cell types using RT-PCR (Fig. 4B). The primers used in RT-PCR study, which are specific for MRP1, were previously used to demonstrate MRP1 expression in cell lines derived from placenta, liver, and lung (25).

Previous studies suggested the presence of a probenecid-sensitive and metabolic energy-dependent organic anion transporter for the entry of anions into the RPE cells (2). However, there are no such reports with the ARPE-19 cells used in this study. Our temperature and metabolic inhibitor studies with ARPE-19 cells supported the possibility of an active entry mechanism for fluorescein, while indicating an additional temperature-independent passive uptake mechanism (Fig. 1). If fluorescein is taken up exclusively by a passive mechanism, upon inhibition of the active efflux mechanism at low temperature, an increase in the cellular accumulation of fluorescein is anticipated. However, at low temperature, there was a decrease in fluorescein accumulation in ARPE-19 cells (Fig. 1), suggesting that fluorescein enters these cells in part by a temperature-dependent mechanism. Also, the cellular accumulation of fluorescein at low temperature was significant, with the accumulation being 40% or higher compared to 37°C. Thus, there is substantial entry of fluorescein into ARPE-19 cells by a temperature-independent passive mechanism as well. Similarly, BAPSG exhibited significant cellular accumulation at low temperature (Fig. 5), with an additional temperature-dependent component.

Energy depleting dinitrophenol and sodium azide elevated solute accumulation only when fluorescein and BAPSG were tested at low concentrations. The effects of these agents are more difficult to interpret as they may perturb the cells besides inhibiting energy-dependent entry as well as efflux mechanisms. Also, some inhibitors of MRP besides inhibiting MRP-mediated anion efflux may inhibit organic anion entry into cells. For instance, probenecid can inhibit organic anion entry as well as efflux. It is conceivable that in such an instance, low probenecid concentrations may inhibit entry while high concentrations may inhibit efflux. Possibly for this reason, relatively high concentrations of probenecid were required to elevate the accumulation of fluorescein (Fig. 2B and 2E) and BAPSG (Fig. 6B) in RPE cells.

Between fluorescein and BAPSG, fluorescein appears to be a better substrate for MRP. Mean fluorescein efflux from ARPE-19 cells in controls at the end of 3 h was 46 ng/mg protein (Fig. 3) compared to a 3-h initial accumulation of 68 ng/mg protein (Fig. 2A). Thus, about 68% of fluorescein was

Table I. Effect of 6-hour MRP Inhibitor Treatment on the Viability of ARPE-19 cells

Treatment	Relative toxicity[a]
Assay buffer with fluorescein (100 µM)	100 ± 20%
Indomethacin (100 µM)	95 ± 13%
Probenecid (1000 µM)	89 ± 12%
Verapamil (100 µM)	92 ± 24%

[a] Data is expressed as mean ± S.D. for $n = 4$. There was no statistically significant difference between different groups at $p < 0.05$.

effluxed in 3 h. On the other hand, BAPSG efflux in 3 h was 24%, as the 3-h BAPSG efflux in controls was 34 ng/mg protein (Fig. 7) compared to a 3-h accumulation of 140 ng/mg protein (Fig. 6). Even with lower concentrations of inhibitors, we were able to better discern MRP functional activity using efflux studies (Fig. 3 and 7) compared to accumulation studies (Fig. 2 and 6). This can in part be due to the fact that efflux studies allow the study of exit mechanism without interfering with the entry mechanism of the anionic solutes. Such an interference with the entry mechanism is likely during accumulation studies where the drug and inhibitor are co-exposed to the cells.

As functional, western blot and RT-PCR studies indicated the activity and expression of MRP in ARPE-19 cells, we used this model to study the interaction of BAPSG, a novel ARI, with MRP. BAPSG belongs to the class of substituted glycine derivatives with high *in vitro* activity against aldose reductase (15). Among a series of related potent ARIs screened, corneal and conjunctival permeability was the highest for BAPSG (28). However, BAPSG has low availability in the posterior segment of the eye following topical administration (19). In this study, we observed an increase in BAPSG accumulation (Fig. 6) and a decrease in efflux (Fig. 7) in ARPE-19 cells in the presence of MRP inhibitors, suggesting that this is a likely approach to enhance retinal delivery of BAPSG. Thus, this study provided the first evidence for the presence of MRP1 in retinal pigment epithelium and further identified a novel aldose reductase inhibitor, BAPSG, which interacts with MRP.

ACKNOWLEDGMENTS

The authors are grateful to Dr. Donald Miller, UNMC School of Pharmacy, for critically reviewing the manuscript and for providing PANC-1 Cells. We are thankful to Dr. Jack DeRuiter and Dr. Randall Clark of Auburn University for their assistance in the synthesis of BAPSG.

REFERENCES

1. B. A. Hughes, R. P. Gallemore, and S. S. Miller. Transport mechanisms in the retinal pigment epithelium. In M. F. Marmor, and T. J. Wolfenberger (eds.), *The Retinal Pigment Epithelium Function and Disease.* Oxford University Press, New York, 1998 pp. 103–135.
2. S. Koyano, M. Araie, and S. Eguchi. Movement of fluorescein and its glucuronide across retinal pigment epithelium-choroid. *Invest. Ophthalmol. Vis. Sci.* **34**:531–538 (1993).
3. E. Bakos, T. Hegedus, Z. Hollo, E. Welker, G. E. Tusnady, G. J. Zaman, M. J. Flens, A. Varadi, and B. Sarkadi. Membrane topology and glycosylation of the human multidrug resistance-associated protein. *J. Biol. Chem.* **271**:12322–12326 (1996).
4. M. Kool, M. de Haas, G. L. Scheffer, R. J. Scheper, M. J. Van Eijk, J. A. Juijn, F. Baas, and P. Borst. Analysis of expression of cMOAT (MRP2), MRP3, MRP4, and MRP5, homologues of multidrug resistance-associated protein gene (MRP1) in human cancer cell lines. *Cancer Res.* **57**:3537–3547 (1997).
5. M. Kool, M. van der Linden, M. de Haas, F. Baas, and P. Borst. Expression of human MRP6, a homologue of multidrug resistance protein gene MRP1 in tissues and cancer cells. *Cancer Res.* **59**:175–182 (1999).
6. Z. Hollow, L. Homolya, T. Hegedus, and B. Sarkadi. Transport properties of the multidrug resistance-associated protein (MRP) in human tumor cells. *FEBS Lett.* **383**:99–104 (1996).
7. Y. Zhang, H. Han, W. F. Elmquist, and D. W. Miller. Expression of various multidrug resistance protein (MRP) homologues in brain microvessel endothelial cells. *Brain Res.* **876**:148–153 (2000).
8. V. V. Rao, J. L. Dahlheimer, M. E. Bardgett, A. Z. Snyder, R. A. Finch, Sartorelli, and W. D. Piwnica. Choroid plexus epithelial expression of MDR1 P-glycoprotein and multidrug resistance-associated protein contribute to the blood-cerebrospinal-fluid-permeability barrier. *Proc. Natl. Acad. Sci. USA.* **96**:3900–3905 (1999).
9. H. Huai-Yun, D. T. Secrest, K. S. Mark, D. Carney, C. Brandquist, W. F. Elmquist, and D. W. Miller. Expression of multidrug resistance-associated protein (MRP) in brain microvessel endothelial cells. *Biochem. Biophys. Res. Commun.* **243**:816–820 (1998).
10. K. C. Dunn, A. E. Aotaki-Keen, F. R. Putkey, and L. M. Hjelmeland. ARPE-19, a human retinal pigment epithelial cell line with differentiated properties. *Exp. Eye Res.* **62**:155–169 (1996).
11. K. C. Dunn, A. D. Marstein, V. L. Bonilha, E. Rodriguez-Boulan, F. Giordano, and L. M. Hjelmeland. Use of the ARPE-19 cell line as a model of RPE polarity: Basolateral secretion of FGF5. *Invest. Ophthalmol. Vis. Sci.* **39**:2744–2749 (1998).
12. G. M. Holtkamp, M. van Rossem, A. F. de Vos, B. Willekens, R. Peek, and A. Kijlstra. Polarized secretion of IL-6 and IL-8 by human retinal pigment epithelial cells. *Clin. Exp. Immunol.* **112**: 34–43 (1998).
13. R. N. Frank, R. Amin, A. Kennedy, and T. C. Hohman. An aldose reductase inhibitor and aminoguanidine prevent vascular endothelial growth factor expression in rats with long-term galactosemia. *Arch. Ophthalmol.* **115**:1036–1047 (1997).
14. M. Lu, S. Amano, K. Miyamoto, R. Garland, K. Keough, W. Qin, and A. P. Adamis. Insulin-induced vascular endothelial growth factor expression in retina. *Invest. Ophthalmol. Vis. Sci.* **57**:584–589 (1999).
15. J. DeRuiter, A. N. Brubaker, M. A. Garner, J. M. Barksdale, and C. A. Mayfield. *In vitro* inhibitory activity of substituted N-benzenesulfonylglycine derivatives. *J. Pharm. Sci.* **76**:149–152 (1987).
16. U. B. Kompella, J. V. Aukunuru, G. Sunkara, and S. P. Ayalasomayajula. Influence of oxygen free radicals, 4-hydroxynonenal, 15-HETE, and aldose reductase pathway on vascular endothelial growth factor secretion from human retinal pigment epithelial cells. *Invest. Ophthalmol. Vis. Sci.* **41**:S772 (2000).
17. D. W. Miller, E. V. Batrakova, and A. V. Kabanov. Inhibition of multidrug resistance-associated protein (MRP) functional activity with pluronic block copolymers. *Pharm. Res.* **16**:396–401 (1999).
18. W. B. Thoreson, B. N. Khandalavala, R. G. Manahan, I. A. Polyak, J. L. Liu, and D. M. Chacko. Lysophosphatidic acid stimulates proliferation of human retinal pigment epithelial cells. *Curr. Eye Res.* **16**:698–702 (1997).
19. G. Sunkara, J. DeRuiter, C. R. Clark, and U. B. Kompella. In-vitro hydrolysis, permeability, and ocular uptake of Prodrugs of N-[4-(benzoylamino) phenylsulfonyl]glycine, a novel aldose reductase inhibitor. *J. Pharm. Pharmacol.* **52**:1113–1122 (2000).
20. D. W. Miller, M. M. Fontain, C. Kolar, and T. Lawson. The expression of multidrug resistance-associated protein (MRP) in pancreatic adenocarcinoma cell lines. *Cancer Lett.* **107**:301–306 (1996).
21. M. P. Draper, R. L. Marter, and S. B. Levy. Indomethacin-mediated reversal of multidrug resistance and drug efflux in human and murine cell lines over expressing MRP, but not P-glycoprotein. *Br. J. Cancer.* **76**:810–815 (1997).
22. S. Gollapudi, C. H. Kim, B. N. Tran, S. Sangha, and S. Gupta. Probenecid reverses multidrug resistance in multidrug resistance associated-protein-overexpressing HL60/AR, H69/AR cells but not in P-glycoprotein-over expressing HL60/Tax and P388/ADR cells. *Cancer Chemother. Pharmacol.* **40**:150–158 (1997).
23. W. Berger, L. Elbling, E. Hauptmann, and M. Micksche. Expression of the multidrug resistance-associated protein (MRP) and chemoresistance of human non-small-cell lung cancer cells. *Int. J. Cancer* **73**:84–93 (1997).
24. M. A. Barrand, T. Rhodes, M. S. Center, and P. R. Twentyman. Chemosensitization and drug accumulation effects of cyclosporin A, PSC-833 and verapamil in human MDR large cell lung cancer cells expressing a 190 kD membrane protein distinct from P-glycoprotein. *Eur. J. Cancer* **29**:408–415 (1993).
25. L. Pascolo, C. Fernetti, P. Doroti, B. Samanta, V. G. Maria, A. Spano, D. Puzzer, C. Tiribelli, A. Amoroso, and S. Crovella.

Detection of MRP1mRNA in human tumors and tumor cell lines by *in situ* RT-PCR. *Biochem. Biophys. Res. Commun.* **275**:466–471 (2000).
26. H. Sun, D. W. Miller, and W. F. Elmquist. Organic anion transport in the central nervous system: A study of fluorescein CNS distribution kinetics. *PharmSci* **2**:1321 (2000).
27. G. L. Scheffer, M. Kool, M. Heijn, M. de Haas, A. C. Pijnenborg, J. Wijnholds, A. van Helvoort, M. C. de Jong, J. H. Hooijberg, C. A. Mol, M. van der Linden, J. M. de Vree, R. P. Elferink, P. Borst, R. J. Scheper. Specific detection of multidrug resistance proteins MRP1, MRP2, MRP3, MRP5, and MDR3 P-glycoprotein with a panel of monoclonal antibodies. *Cancer Res.* **60**:5269–5277 (2000).
28. U. B. Kompella, G. Sunkara, E. Thomas, C. R. Clark, and J. DeRuiter. Rabbit corneal and conjunctival permeability of the novel aldose reductase inhibitors: N-[4-(benzoylamino)phenyl] sulphonyl glycines and N-benzyoyl-N-phenyl glycines. *J. Pharm. Pharmacol.* **51**:921–927 (1999).